

1 Frontal and parietal alpha oscillations reflect 2 attentional modulation of cross-modal matching

3
4 Jonas Misselhorn^{1*}, Uwe Frieze^{1,2}, & Andreas K. Engel¹

5
6 ¹University Medical Center Hamburg-Eppendorf, Department of Neurophysiology and Pathophysiology,
7 Hamburg, Germany

8 ²University of Osnabrück, Institute of Cognitive Science, Osnabrück, Germany

9
10 *Correspondence: j.misselhorn@uke.de

13 Abstract

14 Multisensory perception is characterised by attentional selection of relevant sensory inputs and
15 exploitation of cross-modal similarities that promote cross-modal binding. Underlying
16 mechanisms of both top-down and bottom-up modulations have been linked to changes in
17 alpha/gamma dynamics in primary sensory cortices. Accordingly, it has been proposed that
18 alpha oscillations provide pulsed inhibition for gamma activity and thereby dynamically route
19 cortical information flow. In this study, we employed a recently introduced multisensory
20 paradigm incorporating both bottom-up and top-down aspects of cross-modal attention in an
21 EEG study. The same trimodal stimuli were presented in two distinct attentional conditions,
22 focused on visual-tactile or audio-visual components, for which cross-modal congruence of
23 amplitude changes had to be evaluated. Neither top-down nor bottom-up cross-modal attention
24 modulated alpha or gamma power in primary sensory cortices. Instead, we found alpha band
25 effects in bilateral frontal and right parietal cortex. We propose that frontal alpha oscillations
26 reflect the origin of top-down control regulating perceptual gains and that parietal alpha relates
27 to sensory re-orienting. Taken together, we suggest that the idea of selective cortical routing
28 via alpha oscillations can be extended from sensory cortices to the fronto-parietal attention
29 network.

32 Acknowledgements

33 This work was supported by grants from the German Research Foundation (SFB 936/A3 and
34 SFB TRR 169/B1 to A.K.E. as well as DFG FR-3366-1 to U.F.), the EU (ERC-2010-AdG-
35 269716 to A.K.E.) and the Landesforschungsförderung Hamburg (CROSS FV 25 to A.K.E.).
36 We thank Bettina Schwab for invaluable discussions on the manuscript and Nina Noverijan for
37 assistance in data recording.

38 Author contributions

39 J.M., U.F. and A.K.E. designed the experiment. J.M. recorded the data. J.M. analysed the data.
40 J.M. wrote the main manuscript text. J.M., U.F. and A.K.E. reviewed the manuscript.

43 Competing Interests

44 The authors declare that they have no competing interests.

46 Data Availability

47 Behavioural and electrophysiological data will be made available upon request to the
48 corresponding author.

49

Introduction

50 Human perception is governed by constant influx of information through multiple
51 sensory channels. The act of perceiving routes information flow by active engagement with the
52 multisensory environment, causing sensory inputs to be constantly shaped by modulatory
53 signals reflecting behavioural goals, contextual demands and structural properties of the
54 environment. Spotting a singing bird in a tree, for instance, does not depend on tactile
55 processing but on evaluating visual and auditory signals for temporo-spatial congruence.
56 Lacing shoes, on the other hand, makes little use of audition but integrates vision and tactile
57 perception in a goal-directed manner. These examples illustrate that multisensory perception is
58 shaped by top-down and bottom-up modulation of sensory inputs. Attempts to understand
59 multisensory perception accordingly need to address neural mechanisms underlying both
60 selection of relevant sensory input and exploitation of cross-modal similarities that promote
61 cross-modal binding.

62 A well-described mechanism of stimulus selection via attentional modulation is gain
63 regulation of population responses in sensory regions^{1,2}. In MEG and EEG studies, these gain
64 regulations are likely reflected in alpha band dynamics³. Jensen and Mazaheri⁴ propose that
65 alpha band activity plays a general role in the up- and down-regulation of cortical processing
66 capabilities (“gating by inhibition”). By pulsed inhibition, alpha oscillations could effectively
67 gate gamma band activity related to active processing⁵. This has been shown repeatedly in the
68 context of spatial attention^{6,7,8} while evidence supporting its applicability to cross-modal
69 attention is sparse^{9,10}. Additionally, it is unclear whether pulsed inhibition regulates cortical
70 processing beyond sensory cortices, for instance in cortical regions exerting top-down control.

71 Mechanisms underlying stimulus-driven cross-modal binding are less well understood.
72 In fact, it remains a matter of debate at what stage of cortical processing such interactions take
73 place^{11,12,13}. While some evidence suggests that input to distinct modalities is processed in
74 parallel and only converges later in regions of the temporal and parietal lobe^{14,15,16}, other
75 evidence points out that interactions can already take place at the level of primary sensory
76 regions^{17,18,19}. The disparity of findings is not surprising given that factors driving cross-modal
77 integration span from psychophysical (spatial/temporal congruence) to memory-dependent
78 (semantic congruence and cross-modal correspondences). Yet, a linking observation is that low-
79 and high-level integration have been associated with changes in gamma band activity^{13,20,21}.

80 In the EEG study reported here, we employed a recently introduced multisensory
81 paradigm incorporating both bottom-up and top-down aspects of cross-modal attention²². This
82 paradigm involved a trimodal stimulus consisting of a visual, an auditory and a tactile

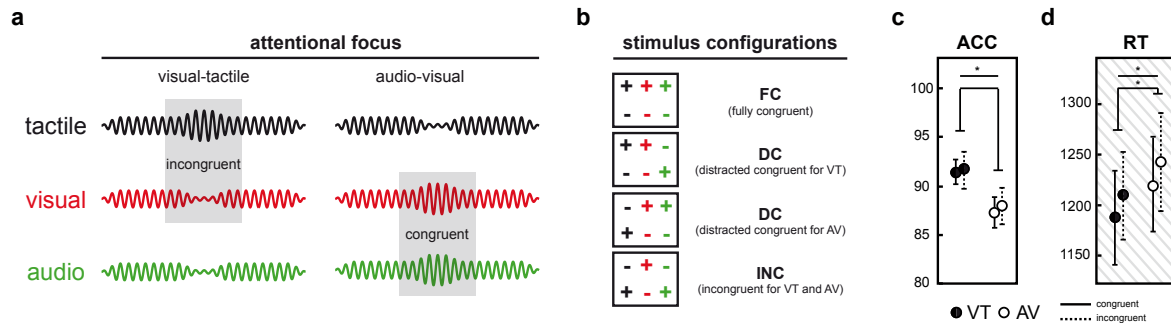


Figure 1: Schematic of matching task and behavioural results. **a**) Illustration of example trials in the two attentional conditions. Under visual-tactile focus (left), the changes in the target stimuli are incongruent, as the tactile stimulus (black) increases in intensity while the visual stimulus (red) decreases. Under audio-visual focus (right), target change is congruent, since visual and auditory (green) stimuli both increase in intensity. **b**) In each block, all possible stimulus configurations occurred with equal probability. Intensity changes are depicted by coloured plus/minus signs (colour coding as introduced in a)). **c**) Accuracy (ACC) in percentage correct. Error bars represent standard deviations. There was no effects of experimental conditions. **d**) Reactions times in milliseconds (RTs). Error bars represent standard deviations. *ATTENTION* as well as *CONGRUENCE* significantly affected the timing of responses, but not the accuracy of responding (Note: RTs were collected in a previous behavioural study²¹ from the same sample of participants).

83 component that each underwent a brief increase or decrease in intensity. Participants had to
 84 attend two of the stimuli and had to decide whether the attended pair changed congruently or
 85 incongruently. In a similar study investigating audio-visual matching with MEG, changes in
 86 primary sensory alpha and gamma activity were more profound when participants attended
 87 presentations compared to when they were ignored¹⁰. In order to further investigate whether
 88 this modulation of alpha/gamma band dynamics holds in situations where attention is not
 89 holistic but rather modality-based, we presented the same trimodal stimuli in two distinct
 90 attentional conditions (top-down), focused on either visual-tactile (VT) or audio-visual (AV)
 91 components, for which cross-modal congruence (bottom-up) of amplitude changes had to be
 92 evaluated (Fig. 1 a). We expected top-down cross-modal attention to selectively enhance
 93 primary sensory alpha activity for irrelevant modalities and decrease alpha activity for attended
 94 modalities. This increase/decrease in alpha power might be accompanied by a decrease/increase
 95 in gamma band activity. As a bottom-up effect of cross-modal binding, gamma band activity
 96 in sensory cortices or temporal/parietal cortex is expected to be modulated by cross-modal
 97 congruence.

98 Results

99 Psychophysics and behaviour

100 The trimodal stimulus material was designed such that the target amplitude changes in
 101 each modality were equally salient. This was achieved by estimating detection thresholds for
 102 each modality and change direction separately using a psychophysical staircase procedure²³.
 103 Yet, a questionnaire that was completed during debriefing of a preceding behavioural study²²

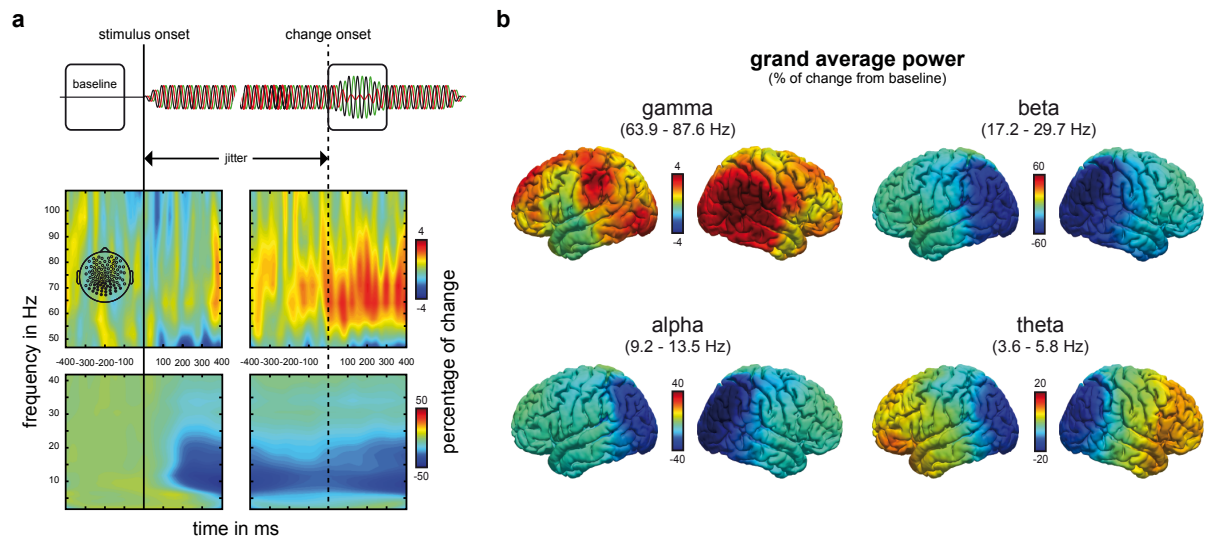


Figure 2: Average time-frequency dynamics in sensor and source space. a) Time-frequency dynamics in sensor space at occipito-parietal channels (topography shown in upper left panel), time locked to stimulus onset (left panels, black solid vertical line) and change onset (right panels, black dashed vertical line). **Top:** Schematic of temporal trial structure displaying the two relevant time-windows used for analysis: a baseline (-400:-100 ms) separated by a jitter (stimulus to change onset between 700 and 1000 ms) from the change interval (0:300 ms). **Bottom:** Time-frequency plots from posterior sensors. Values represent percentage of change from baseline. **b)** Distribution of band-limited power on the cortical surface in the change interval relative to baseline.

104 indicated that subjective salience of the sensory components was in fact not equal but strongest
105 for the visual component. In particular, participants reported that the visual component was
106 hardest to ignore when it was task irrelevant (pairwise Wilcoxon rank sum test, Bonferroni
107 corrected, V-T: $p = .002$, V-A: $p = .24$, T-A: $p = .26$). This should be kept in mind for the
108 discussion of the effects of cross-modal attention.

109 The timing and accuracy of responding was analysed with a repeated measure analysis
110 of variance (ANOVA) with factors *ATTENTION* (VT vs. AV) and *CONGRUENCE* (congruent
111 vs. incongruent). Responses were faster but not more accurate when subjects attended cross-
112 modally congruent pairs (Fig. 1 d; $p < .001$, $\eta_p^2 = 0.471$). When participants attended VT, timing
113 as well as accuracy of responding was significantly better compared with the AV conditions
114 (RT: $p = .036$, $\eta_p^2 = 0.201$; ACC: $p = .005$, $\eta_p^2 = 0.327$). No interaction effects between
115 *ATTENTION* and *CONGRUENCE* were observed.

116 ROI analysis

117 In Figure 2, we present an overview of time-frequency dynamics during the task as well
118 as distributions of band-limited power for theta, alpha, beta and gamma bands in source space.
119 In order to investigate power changes in oscillatory activity in primary sensory areas occurring
120 after the stimulus increases or decreases, we conducted a regions of interest (ROI) analysis on
121 source projected EEG data in primary visual, auditory and somatosensory cortex. Statistical
122 evaluation was carried out with a repeated measures ANOVA with factors *ROI*, *ATTENTION*

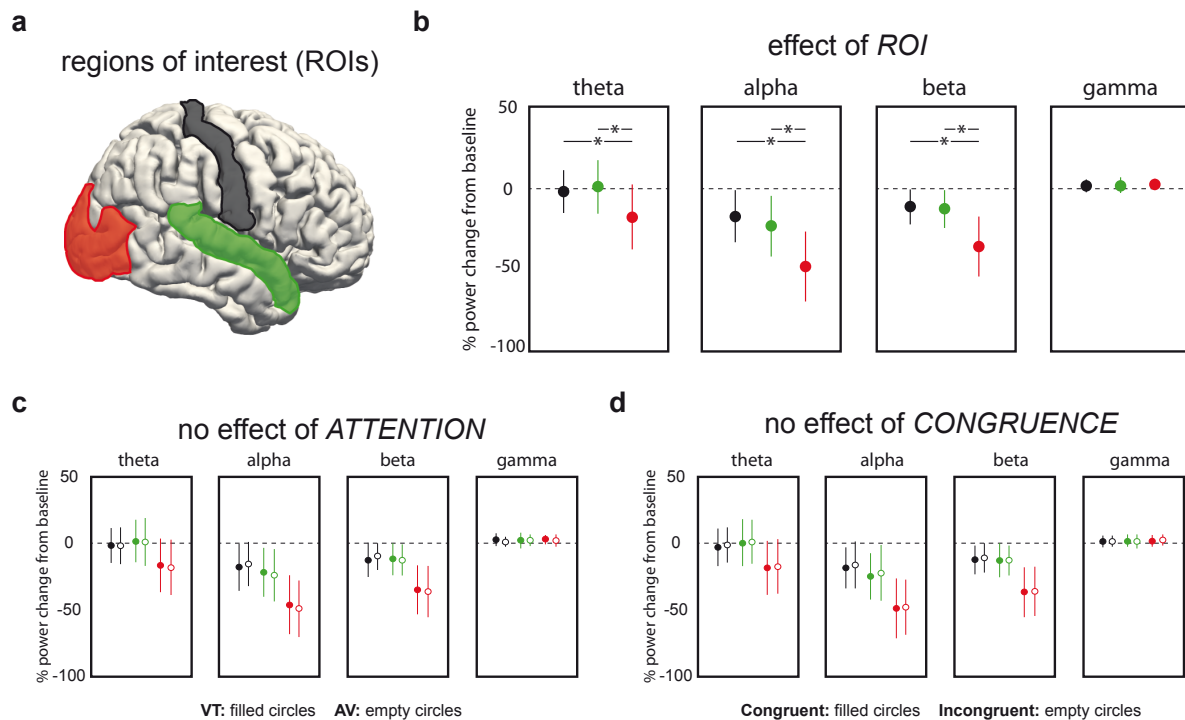


Figure 3: Regions of interest (ROI) analysis of band-limited power during change epoch in primary sensory areas. a) Primary sensory areas used for ROI ANOVA with factors *ATTENTION* (VT vs. AV), *CONGRUENCE* (congruent vs. incongruent) and *ROI* (visual vs. auditory vs. somatosensory); visual = red, auditory = green, somatosensory = black. **b)** Effect of *ROI* is significant for theta, alpha and beta bands, but not gamma band. Asterisk signifies significant comparisons ($p < .001$). **c)** No significant effect of *ATTENTION*. **d)** No significant effect of *CONGRUENCE*.

123 and *CONGRUENCE* separately for each frequency band (Fig. 3, see *Methods* for details).
 124 Significant effects of *ROI* were observed for theta, alpha and beta bands (for all, $p < .001$ and
 125 $\eta_p^2 > 0.5$; see Fig. 3 b). In the gamma band, *ROI* did not explain a significant amount of variance
 126 ($p = .689$). Simple effects analysis for the lower frequency bands showed that decreases in
 127 power were significantly stronger in visual compared with both auditory and somatosensory
 128 ROIs (for all comparisons, $p < .001$; Fig. 3 b). Power changes in auditory and somatosensory
 129 ROIs did not differ (for all, $p > .05$). The main effects and interactions of *ATTENTION* and
 130 *CONGRUENCE* were not significant (for all, $p > .05$; Fig. 3 c + d).

131 Cluster statistics

132 To complement the ROI analysis, we conducted a whole-brain analysis of task-related
 133 power changes in the interval after stimulus increases and decreases evaluated by means of
 134 nonparametric cluster-based permutation statistics (see *Methods* for details). For the
 135 *ATTENTION* contrast (VT minus AV), significant differences were found in the alpha band. In
 136 two roughly symmetric clusters, VT attention was associated with stronger power decrease of
 137 alpha oscillations when compared with AV attention (Fig. 4 a). In the left hemisphere, the
 138 cluster was situated in the border region of pre-central gyrus, middle frontal gyrus (MFG) and

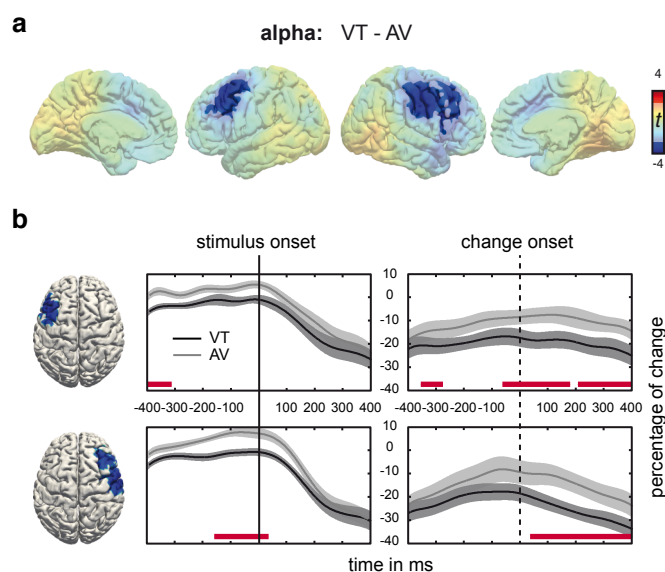


Figure 4: Effect of ATTENTION (VT - AV). **a**) Cluster-based permutation statistic of the contrast VT *minus* AV in the alpha band during change interval. T-values of the respective contrasts are depicted. Shaded voxels are non-significant. **b**) Time-course of alpha activity within significant clusters. Shading corresponds to the standard error of the mean. Red bars indicate temporal regions of significance as determined by permutation testing (see *Methods* for details).

139 superior frontal gyrus encompassing the frontal eye fields (FEF; $p = .031$). In the right
 140 hemisphere, the cluster was situated similarly but expanded further into pre- and post-central
 141 gyrus ($p = .005$). In a next step, we analysed time courses of alpha power modulations within
 142 these two clusters (Fig. 4 b, see *Methods*). Throughout the entire time course, alpha power was
 143 lower for VT than for AV attention. This difference was significant before stimulus onset in
 144 both hemispheres (left: [-400; -312] ms, right: [-165; 43] ms), in a short epoch prior to change
 145 onset in the left hemisphere ([-348; -286] ms) and throughout the whole change epoch in both
 146 hemispheres (left: [-69; 177] ms and [211; 400] ms, right: [43; 400] ms).

147 When evaluating the effect of *CONGRUENCE* (attended congruent *minus* attended
 148 incongruent), significant differences were found in alpha and theta bands (Fig. 5). Theta power
 149 was higher for congruent trials compared to incongruent trials in large parts of the medial wall
 150 of both hemispheres (Fig. 5 a). This effect was significant in a left hemispheric cluster stretching
 151 from posterior to anterior cingulate cortex. In a next step, we analysed the contributions of fully
 152 congruent (FC) and distracted congruent (DC) trials to the overall effect of congruence (see
 153 Fig. 1 b and *Methods* for details). It was driven by FC trials for which theta power was increased
 154 in cingulate cortex of both hemispheres, and in small clusters in left and right intraparietal
 155 sulcus (IPS) as well as left inferior frontal gyrus (IFG) and right MFG (Fig. 5 c). No significant
 156 theta power differences were seen when comparing distracted congruent with incongruent trials
 157 (Fig. 5 e).

158 In the alpha band, cross-modal congruence modulated power in large parts of medial
 159 and lateral cortex. In incongruent trials, stronger decrements of alpha power occurred in
 160 bilateral medial superior frontal cortex and left MFG (Fig. 5 b). Congruent trials were associated
 161 with stronger decrements in alpha power in bilateral medial occipito-parietal cortex and right

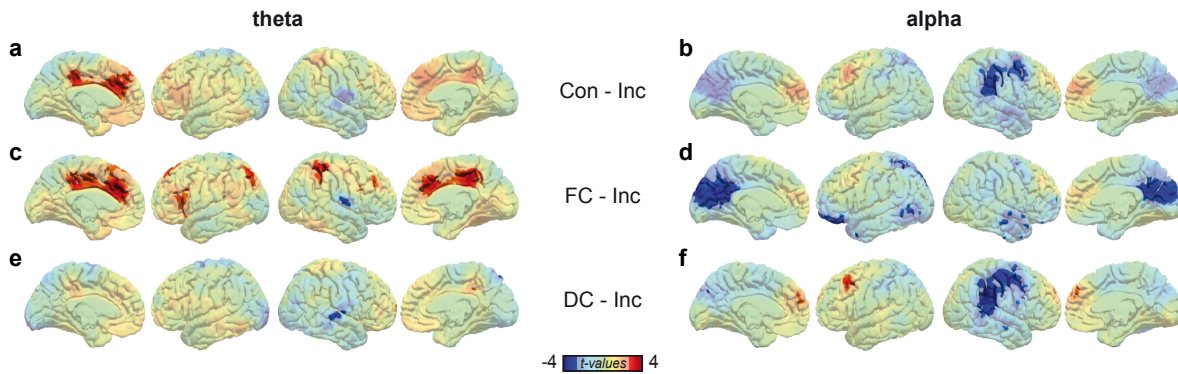


Figure 5. Effect of CONGRUENCE (Congruent - Incongruent). **a+b)** Cluster-based permutation statistic of the contrast *Congruent - Incongruent* in the alpha (a) and theta (b) band during change interval. All subplots depict t-values. Shaded voxels are non-significant. **c)** Contrast between theta power in *fully congruent* (FC) and *incongruent* trials. **d)** Contrast between alpha power in *fully congruent* (FC) and *incongruent* trials. **e)** Contrast between theta power in *distracted congruent* (DC) and *incongruent* trials. **f)** Contrast between alpha power in *distracted congruent* (DC) and *incongruent* trials.

162 inferior parietal and middle frontal cortex. The latter difference was significant in a cluster
163 covering the right temporoparietal junction (TPJ), but stretching rostrally towards right MFG.
164 Next, we disentangled contributions from FC and DC trials as before for theta power. While
165 FC trials significantly drove the effect in medial occipito-parietal cortex (Fig. 5 d), DC trials
166 contributed significantly to the effect in medial and left middle frontal cortex (Fig. 5 e). The
167 effect in right TPJ and MFG was dominated by DC trials (Fig. 5 d).

168 Discussion

169 We investigated bottom-up and top-down modulation of sensory processing in a cross-
170 modal matching task involving visual, auditory and tactile perception. Contrary to our
171 expectations, we did not find alpha/gamma oscillations in primary sensory areas to be
172 modulated by bottom-up or top-down cross-modal attention. This finding is surprising given
173 that both processes have often been noted to be accompanied by alpha/gamma modulations in
174 sensory cortices^{3,6,7,10,18,19}. Our explanation for the lack of primary sensory modulation is the
175 nature of the task: many, if not most, multisensory studies employ detection tasks with near-
176 threshold sensory stimulation. In these situations of low sensory drive, both bottom-up and top-
177 down modulation of sensory input can be expected to have higher impact compared with
178 situations of strong sensory drive. Stimulus-driven cross-modal enhancement by spatio-
179 temporal congruence, for instance, is assumed to obey the law of inverse effectiveness, meaning
180 that there is an inverse relationship between possible cross-modal enhancement and stimulus
181 intensity²⁴. Here, however, all stimulus intensities were clearly supra-threshold with
182 superimposed amplitude changes. Top-down as well as bottom-up modulation of sensory
183 processing might thus be subtle and hence not detectable by EEG. Instead, we found theta
184 oscillations in cingulate cortex and most notably alpha oscillations in frontal and parietal cortex
185 to be modulated. In the following, we propose that frontal alpha oscillations reflect the origin

186 of top-down control regulating perceptual gains and that parietal alpha oscillations relate to
187 sensory (re-)orienting. Theta activity in cingulate cortex is finally discussed in the context of
188 adaptive task-switching behaviour circumventing cross-modal matching.

189 Reduction of alpha power in bilateral FEF and MFG as well as right pre-/post-central
190 gyrus was stronger for VT cross-modal attention compared to AV attention. This difference
191 was significant even before stimulus onset. Besides their role in oculomotor control, the FEF
192 have been described as important structures in top-down attention²⁵. In a study using TMS,
193 Grosbas and Paus showed that disruption of activity in FEF shortly before the onset of the target
194 in a visuospatial covert attention task facilitated responses²⁶. Conversely, 10 Hz TMS over the
195 right FEF was shown to impair visual search of unpredictable items with low salience²⁷. Moore
196 and Armstrong reconciled this conflicting evidence by suggesting that the FEF has a general
197 role in regulating visual gain²⁸. In their study, electric stimulation of FEF in the monkey either
198 enhanced or inhibited responses to visual stimuli in V4 depending on whether retinotopically
199 corresponding sites were stimulated. Studies in humans supported this idea by showing that
200 TMS over FEF could increase phosphene or contrast sensitivity of extrastriate cortex^{29,30}. This
201 top-down modulation of visual cortex was demonstrated even in the absence of sensory input³¹.
202 Likewise, anticipatory alpha and stimulus related gamma activity in occipito-parietal cortex
203 could be modulated by TMS over FEF³². The strength of modulation was shown to correlate
204 with the strength of structural connectivity between frontal and parietal cortex via the superior
205 longitudinal fasciculus³³. Thus, animal and human studies jointly conclude that the FEF can
206 dynamically modulate the gain of down-stream visual cortex independent of sensory input. In
207 our study, FEF/MFG likely facilitated cross-modal matching by modulating visual gain to
208 counter visual dominance. Although stimulus intensity was titrated to be balanced across
209 modalities (see *Methods*), we have reason to assume that perceived salience was highest for the
210 visual component. In a questionnaire that was completed during debriefing of the preceding
211 behavioural study, we asked participants to rank the difficulty to ignore a given modality. Most
212 participants reported that visual components were hardest and tactile components easiest to
213 ignore. This finding is in line with a pattern of sensory dominance found for combinations of
214 visual, auditory and somatosensory stimuli in a discrimination task³⁴. Sensory dominance can
215 be problematic under the assumption that cross-modal matching is not independent of
216 perceptual gain. This is most likely the case for stimulus-driven aspects of multisensory
217 integration – the idea of inverse effectiveness, after all, assumes multimodal stimuli of low but
218 comparable intensity²⁴. Consequentially, decreased power of alpha oscillations in FEF/MFG is
219 taken as evidence for an increased down-regulation of visual gain in VT conditions to account
220 for unequal subjective salience of the stimuli to be matched.

221 As discussed above, balancing perceptual gains across modalities by top-down
222 modulation likely enables optimal use of stimulus-driven aspects of cross-modal matching.
223 These bottom-up factors were ubiquitous in this task; on each trial, participants were
224 simultaneously confronted with three salient events, that is, intensity changes in each modality.
225 Although each change of intensity by itself possessed some degree of bottom-up salience, we
226 suggest that cross-modal congruence amplified salience through cross-modal binding¹³. When
227 cross-modal binding was enhanced between attended modalities, responses were facilitated.
228 This was especially pronounced for fully congruent trials where conflict, and thus the need for
229 actual matching, was absent. All other trials were either distracted congruent (attended
230 modalities change congruently, but the distractor diverged) or attended incongruent (one of the
231 attended modalities is congruent to the distractor). In these cases, cross-modal binding was
232 always stronger between two given modalities compared to the respective third. When
233 contrasting the EEG of these trials, we find alpha band effects in the right temporoparietal
234 junction (rTPJ) and right MFG. Specifically, distracted congruent conditions were associated
235 with decreased power of alpha oscillations in these regions compared with attended incongruent
236 trials. In accordance with the “gating by inhibition” theory, we conclude that the rTPJ/rMFG
237 were more strongly disinhibited when attended modalities had a stronger bottom-up drive for
238 cross-modal binding. The TPJ receives inputs from visual, auditory and somatosensory cortex
239 and is richly connected to temporal and frontal sites, making it an important hub for the
240 interaction of multisensory integration and attention³⁵. Accordingly, lesions to the right TPJ
241 typically result in neglect^{36,37}. A dominant interpretation of rTPJ’s functional role is its
242 involvement in (spatial) re-orienting based on stimulus salience³⁸. In a model integrating goal-
243 directed and stimulus-driven attention, it is suggested that a dorsal network comprising FEF
244 and IPS instantiates attentional sets. As a counterpart, a ventral network comprising rTPJ and
245 right ventral frontal gyrus mediates bottom-up signals acting as a circuit-breaker for the dorsal
246 system. Studies employing multisensory paradigms have noted rTPJ’s involvement in
247 processing cross-modal congruence. In a study investigating visual-tactile pattern matching,
248 pre-stimulus alpha and beta power in right supramarginal gyrus differentiated between
249 detection and congruence-evaluation tasks³⁹. Another study showed that alpha power in right
250 posterior regions was more strongly suppressed during congruent compared with incongruent
251 audio-visual speech presentations⁴⁰. Taken together with our results, we suggest that the rTPJ
252 detects the increased salience of congruent cross-modal events. While each trial might, in
253 principle, result in attentional capture by any of the three modalities, cross-modal binding by
254 congruence might serve as a reliable “cue” for re-orienting towards the relevant modalities.
255 Thereby, cross-modal binding between attended modalities might support modality-based re-
256 orienting.

257 As pointed out above, fully congruent trials were characterised by the absence of cross-
258 modal conflict. In the EEG, these highly salient trials were associated with stronger alpha power
259 reductions in medial occipito-parietal cortex. In an event-related potentials study featuring
260 visual, auditory and somatosensory stimuli, RT facilitation was correlated with the latency of
261 the P300, which was localised in precuneus⁴⁰. Other research suggests that alpha power
262 reductions in occipito-parietal cortex and P300 dynamics are functionally coupled⁴¹. Here,
263 enhanced involvement of medial occipito-parietal cortex is proposed to reflect increased
264 bottom-up salience due to multisensory enhancement, i.e., increased perceptual gains of
265 concurrent congruent sensory input to more than one modality⁴². In addition to mere bottom-
266 up sensory salience, fully congruent stimuli occurred in only 25 % of all trials and were thereby
267 salient. Actual cross-modal matching was required only in the remaining 75 % of trials where
268 two modalities changed congruently while the third modality diverged. An efficient strategy
269 would accordingly be to “switch” between these two tasks, i.e., between detecting highly salient
270 events and cross-modal matching of conflicting input. In addition to the alpha band effect in
271 precuneus, fully congruent trials were also associated with a relative increase in theta power in
272 bilateral cingulate cortex. Theta band activity in cingulate cortex has previously been related to
273 the adjustment of stimulus response mappings⁴³. Together with insular cortex, cingulate cortex
274 is part of a salience network which has importance for both bottom-up detection of salient
275 events and switching between large-scale networks to adaptively control behaviour⁴⁴. Here, it
276 is suggested that reduced alpha power in medial occipito-parietal cortex related to multisensory
277 enhancement acts as a salience signal detected by cingulate cortex which in turn initiates
278 adaptive task-switching behaviour.

279 Taken together, we provide evidence that cross-modal matching in complex
280 multisensory environments heavily relies on mechanisms of attention. Our results contrast with
281 the majority of studies on multisensory integration concerned with stimulus detection where
282 attentional load is typically low. Here, participants were confronted with a highly challenging
283 multisensory setting. In order to counter the bias imposed by visual dominance, top-down
284 regulation of perceptual gains likely supported an optimal exploitation of cross-modal
285 similarities that promote perceptual binding. This was associated with decreased alpha band
286 power in frontal cortices proposed to reflect the origin of top-down modulation. Likewise,
287 bottom-up drive for cross-modal binding was related to changes in alpha power in right parietal
288 cortex proposed to represent the bottom-up modulatory signal underlying sensory re-orienting.
289 Both findings provide evidence for an extension of the idea that alpha/gamma dynamics
290 indicate selective cortical routing beyond sensory cortex to the fronto-parietal attention
291 network.

292

Methods

293 **Participants**

294 Twenty-one participants entered the study and received monetary compensation for
295 their participation. They were on average 23.8 ± 2.5 years old and 11 of them were female (10
296 male). Vision, audition and tactile perception were normal and none of them had a history of
297 neurological or psychiatric disorders. After an explanation of the experimental procedure,
298 participants gave written consent. The ethics committee of the University Medical Center
299 Hamburg-Eppendorf approved the study which was carried out in accordance with the
300 declaration of Helsinki.

301 **Experimental design**

302 On each trial, we presented a trimodal stimulus consisting of a visual, an auditory and a
303 tactile component that each underwent a brief increase or decrease in intensity (see *Stimulus*
304 *Material* for details). Block-wise, participants attended either visual-tactile (VT) or audio-
305 visual (AV) bimodal pairs and ignored the respective third component. The task was to decide
306 whether the attended bimodal pairs changed congruently (i.e., in the same direction) or
307 incongruently (i.e., in different directions; see Fig. 1 a). Verbal responses had to be withheld
308 until stimulus offset to minimise myogenic artifacts. Therefore, reaction times (RTs) could not
309 be evaluated. Instead, we present RT data of the same sample of participants from the
310 behavioural study preceding the EEG study²². In each block, all possible eight stimulus
311 configurations of increases and decreases across modalities were presented with equal
312 probability (Fig. 1 b). VT and AV blocks containing 64 trials presented in randomised order
313 were alternating. Data were collected on two separate days with identical experimental
314 procedure so that EEG data of 1280 trials was collected from each participant. Prior to statistical
315 analysis, trials were pooled without taking change direction into account. For instance, fully
316 congruent trials were both trials where all modalities underwent decrements and trials where
317 all modalities underwent increments (Fig. 1 b, pooling is indicated by boxes).

318 **Stimulus material**

319 Visual contrast, auditory loudness and vibration strength were experimentally increased
320 or decreased. The magnitudes of change per modality and direction were individually estimated
321 prior to the experimental sessions using the same psychometric step function as described in
322 Misselhorn et al. (QUEST)^{22,23}. Intensity changes had a duration of 300 ms and onsets were
323 jittered across trials between 700 and 1000 ms after stimulus onset (Fig. 2 a). In total, sensory
324 stimulation had a fixed duration of 2 s. As visual stimulation, an expanding circular grating was
325 centrally presented against a grey background on a CRT screen with a visual angle of 5°. The

326 auditory component consisted of a complex sinusoidal tone (13 sine waves: 64 Hz and its first
327 6 harmonics as well as 91 Hz and its first 5 harmonics, low-frequency modulator: 0.8 Hz) played
328 back with audiometric insert earphones binaurally at 70 dB (E-A-RTONE 3A, 3M, USA). As
329 tactile stimulation, high-frequency vibrations (250 Hz on C2 tactors, Engineering Acoustics
330 Inc., USA) were delivered to the tips of both index fingers.

331 **EEG**

332 EEG was recorded from 128 active electrodes (Easy Cap, Germany) including four
333 ocular electrodes referenced to the nose. Data was sampled at 1000 Hz with an amplitude
334 resolution of 0.1 μ V using BRAINAMP MR amplifier (Brain Products, Germany) and digitised
335 after analog filtering (low cutoff: 10 s, high cutoff: 1000 Hz). Offline, data was down-sampled
336 to 500 Hz and digitally filtered (high-pass: 1 Hz, low-pass: 120 Hz, notch: 49-51 Hz, 99-101
337 Hz). Epochs of 2.5 s were cut from -500 ms relative to stimulus onset until stimulus offset and
338 normalised to the pre-stimulus baseline. Next, data was re-referenced to the common average
339 and linear trends were removed from all epochs. From the four ocular channels, two bipolar
340 channels for horizontal and vertical eye movements were derived.

341 **Pre-processing.** Trials with incorrect answer and large non-stereotypical artifacts were
342 excluded from further processing. Subsequently, independent component analysis (ICA) was
343 performed separately for low and high frequency bands (low band: 1-30 Hz, high band: 30-120
344 Hz). Thereby, stereotypical low-frequency artifacts (for instance eye movements and heart beat)
345 and high-frequency artifacts (i.e. myogenic activity) could be separated more reliably from
346 neuronal activity. For both bands, principal components analysis was performed first to reduce
347 data such that 99 % of variance is retained. Subsequently, ICA was performed on the rank-
348 reduced data using the infomax algorithm⁴⁵. Artifactual ICs were identified and rejected with
349 respect to time course, spectrum and sensor topography⁴⁶. For the high band, saccade-related
350 transient potentials were removed additionally⁴⁷. Finally, all epochs were visually inspected
351 and epochs with remaining artifacts were rejected. Furthermore, a subset of 19 electrodes (i.e.
352 most outer facial, temporal and neck electrodes) was excluded from further analysis due to poor
353 signal-to-noise ratio. Lastly, data was stratified such that all conditions in the ensuing analysis
354 hold the same amount of data within subjects. On average, 426 ± 89 trials per participant entered
355 the analysis.

356 **Source reconstruction of band-limited signals.** Cleaned data in low and high bands
357 were joined and epoched with respect to stimulus onset as well as change onset. Prior to filtering
358 data into narrow bands by means of wavelet analysis, event related potentials were subtracted
359 in order to remove phase-locked responses. A family of 40 complex Morlet wavelets w with
360 lengths of 2 s was constructed for logarithmically spaced frequencies between 2 and 120 Hz.

361
$$w(t, f_0) = A * e^{-\frac{t^2}{2\sigma_t^2}} * e^{2\pi f_0 t}$$

362 The number of cycles per wavelet (m) were logarithmically spaced between 3 and 10 and
363 subsequently rounded off. Wavelets were normalised by factor $A = \sigma_t \sqrt{\pi}^{-\frac{1}{2}}$ with $\sigma_t =$
364 $m/2\pi f_0$. Single trial data was convolved with the Morlet wavelets by multiplication in the
365 frequency domain using fast fourier transformation with boxcar windows. Wavelet filtered
366 single trial data was then reconstructed in source space using exact low-resolution brain
367 electromagnetic tomography (eLORETA; regularisation: 0.05)⁴⁸. Lead fields were computed
368 for a three-shell head model⁴⁹. The customised cortical grid was derived from a cortical surface
369 provided by Freesurfer in MNI space by reducing the number of cortical nodes from 270000 to
370 10000⁵⁰. Dipole directions at each node of the cortical grid were estimated by means of singular
371 value decomposition of the trial averaged spectral power individually for all bands and kept
372 constant for all trials of the given participant. Induced power was computed from these source
373 reconstructed band-limited time domain signals. Power in the epoch after change onset was
374 baseline corrected using the baseline of the mean over all conditions from -400 to -100 ms
375 relative to stimulus onset (Fig. 2 a). By visual inspection of the resulting time-frequency
376 landscapes, frequency bands in the theta, alpha, beta and gamma range were chosen
377 individually for each participant (mean values and range in parentheses; theta: 4.7 [3.6; 5.8]
378 Hz, alpha: 11.5 [9.2; 13.5] Hz, beta: 23.0 [17.2; 29.7] Hz, gamma: 78.9 [63.9; 87.6] Hz).
379 Statistical analysis was carried out for the post-change interval ([0; 300] ms) only.

380 **Statistical analysis**

381 **Behaviour.** Accuracy of responding (ACC) within experimental conditions was
382 analysed using a repeated-measures analysis of variance (ANOVA) with factors *ATTENTION*
383 (VT vs. AV) and *CONGRUENCE* (congruent vs. incongruent). The timing of verbal responses
384 was not analysed because subjects were instructed to withhold responses until stimulus offset.
385 Instead, data from the previous behavioural study was re-analysed for the sub-sample of
386 participants enrolled in this EEG study²¹. The same ANOVA as described above for ACCs was
387 evaluated.

388 **EEG: Regions of interest (ROIs) analysis.** Primary cortical regions for vision, audition
389 and tactile perception were chosen from the Freesurfer atlas which is constructed by gyral
390 identification and parcellation based on anatomical landmarks⁵⁰. For each frequency band,
391 baseline-corrected, time and ROI averaged data in the post-change interval was evaluated by
392 means of ANOVA with factors *ROI* (visual vs. auditory vs. somatosensory), *ATTENTION* (VT
393 vs. AV) and *CONGRUENCE* (congruent vs. incongruent) and. Simple effects of significant
394 ANOVA effects were assessed by paired-sample t-tests applying Bonferroni correction.

395 ***EEG: Whole-brain permutation statistics.*** Complementing ROI analysis, a whole brain
396 exploratory analysis of differences between experimental conditions was conducted and
397 evaluated by means of nonparametric cluster-based permutation statistics⁵¹. A null distribution
398 was computed by randomly drawing trials into two sets per subject (300000 permutations). For
399 each node of the cortical grid, a paired-sample t-test was computed between averaged power of
400 the two sets and statistical maps were thresholded ($p < .05$). Significant clusters were found and
401 the size of the largest cluster was noted. This procedure was carried out separately for the four
402 frequency bands. Contrasts corresponding to a 2 (*ATTENTION*) x 2 (*CONGRUENCE*) design
403 were computed and evaluated against the aforementioned null-hypothesis (cut-off: 99th
404 percentile). Reported p -values are Bonferroni-corrected.

405 Cluster statistics were complemented by post-hoc analyses that were designed (1) to
406 detail on the time-course of the *ATTENTION* effect and (2) to disentangle the contributions of
407 sub-conditions to the overall effect of *CONGRUENCE*.

408(1) For clusters showing a significant effect of *ATTENTION*, we computed the time course of
409 average within cluster spectral power separately for visual-tactile and audio-visual conditions.
410 Significance of the difference between time courses was evaluated using nonparametric cluster-
411 based permutation statistics (300000 permutations). For each permutation, time courses were
412 shuffled and paired-sample t-tests between VT and AV were computed for each sample. The
413 number of samples included in the longest temporally continuous cluster of significant
414 difference was noted to form the maximum statistic null distribution. In the original data,
415 periods of significant difference between attentional conditions were considered significant in
416 the temporal domain when they held more samples than the 99th percentile of the null
417 distribution.

418(2) For this analysis we differentiated according to whether attended stimulus components were
419 “fully congruent” or “distracted congruent”. Fully congruent (FC) means that all stimulus
420 components, including the distracting modality, change congruently (that is, all components
421 increased or decreased in intensity; Fig. 1 b, top box). Distracted congruent (DC) means that
422 the distractor’s change direction deviates from the change direction in the attended modalities
423 (Fig. 1 b, middle boxes). In this case, the participant has to resolve the conflict between attended
424 congruence and unattended incongruence. In order to disentangle these two scenarios, we
425 computed contrasts of FC respectively DC against attended incongruent conditions.

426

427

428

429

430

References

- 431 1. Pessoa L., Kastner S. & Ungerleider L. G. Neuroimaging studies of attention: From
432 modulation of sensory processing to top-down control. *J Neurosci.* 23, 3990-3998
433 (2003).
- 434 2. Ling S., Liu T. & Carrasco M. How spatial and feature-based attention affect the gain
435 and tuning of population responses. *Vision Res.* 49, 1194-1204 (2009).
- 436 3. Chaumon M. & Busch N. A. Prestimulus neural oscillations inhibit visual perception
437 via modulation of response gain. *J Cogn Neurosci.* 26, 2514-29 (2014).
- 438 4. Jensen O. & Mazaheri A. Shaping functional architecture by oscillatory alpha activity:
439 gating by inhibition. *Front Hum Neurosci.* 4, 186 (2010).
- 440 5. Osipova D., Hermes D. & Jensen O. Gamma power is phase-locked to posterior alpha
441 activity. *PLoS One.* e3990 (2008).
- 442 6. Worden M. S., Foxe J. J., Wang N. & Simpson G. V. Anticipatory biasing of
443 visuospatial attention indexed by retinotopically specific alpha-band
444 electroencephalography increases over occipital cortex. *J Neurosci.* 20, RC63 (2000).
- 445 7. Siegel M., Donner T. H., Oostenveld R., Fries P., & Engel A. K. Neuronal
446 synchronization along the dorsal visual pathway reflects the focus of spatial attention.
447 *Neuron.* 60, 709-19 (2008).
- 448 8. Foster J. J., Sutterer D. W., Serences J. T., Vogel E. K. & Awh E. Alpha-band
449 oscillations enable spatially and temporally resolved tracking of covert spatial attention.
450 *Psychol Sci.* 28, 929-941 (2017).
- 451 9. Mazaheri A., van Schouwenburg M. R., Dimitrijevic A., Denys D., Cools R. & Jensen
452 O. Region-specific modulations in oscillatory alpha activity serve to facilitate
453 processing in the visual and auditory modalities. *Neuroimage.* 87, 356-62 (2014).
- 454 10. Friese U., Daume JI., Göschl F., König P., Wang P. & Engel A. K. Oscillatory brain
455 activity during multisensory attention reflects activation, disinhibition, and cognitive
456 control. *Sci Rep.* 6, 32775 (2016).
- 457 11. Ghazanfar A. A. & Schroeder C. E. Is neocortex essentially multisensory? *Trends Cogn
458 Sci.* 10, 278-85 (2006).
- 459 12. Koelewijn T., Bronkhorst A. & Theeuwesa J. Attention and the multiple stages of
460 multisensory integration: A review of audiovisual studies. *Acta Psychol.* 134, 372-384
461 (2010).
- 462 13. Senkowski D., Schneider T. R., Foxe J. J., & Engel A. K. Crossmodal binding through
463 neural coherence: implications for multisensory processing. *Trends in Neurosciences.*
464 31, 401-409 (2008).
- 465 14. Bien N., ten Oever S., Goebel R. & Sack A. T. The sound of size: Cross-modal binding
466 in pitch-size synesthesia: A combined TMS, EEG and psychophysics study.
467 *Neuroimage* 59, 663-672 (2012).
- 468 15. Schneider T. R., Debener S., Oostenveld R. & Engel A. K. Enhanced EEG gamma-band
469 activity reflects multisensory semantic matching in visual-to-auditory object priming.
470 *Neuroimage* 42, 1244-54 (2008).
- 471 16. Konen C. S. & Haggard P. Multisensory parietal cortex contributes to visual
472 enhancement of touch in humans: A single-pulse TMS study. *Cereb Cortex* 24, 501-
473 507 (2014).

- 474 17. Cappe C. & Barone P. Heteromodal connections supporting multisensory integration at
475 low levels of cortical processing in the monkey. *Eur J Neurosci.* 22, 2886-2902 (2005).
- 476 18. Senkowski D., Talsma D., Herrmann C. S. & Woldorff M. G. Multisensory processing
477 and oscillatory gamma responses: effects of spatial selective attention. *Exp Brain Res.*
478 166, 411-426 (2005).
- 479 19. Lakatos P., O'Connell M. N., Barczak A., Mills A., Javitt D. C. & Schroeder C. E. The
480 leading sense: Supramodal control of neurophysiological context by attention. *Neuron*
481 64, 419-30 (2009).
- 482 20. van Atteveldt N., Murray M. M., Thut G. & Schroeder C. Multisensory integration:
483 flexible use of general operations. *Neuron* 81, 1240–1253 (2014).
- 484 21. Keil J. & Senkowski D. Neural oscillations orchestrate multisensory processing. *The*
485 *Neuroscientist.* 1-18 (2018).
- 486 22. Misselhorn J., Daume J., Engel A. K. & Fries U. A matter of attention: Cross-modal
487 congruence enhances and impairs performance in a novel trimodal matching paradigm.
488 *Neuropsychologia* 88, 113-122 (2015).
- 489 23. Watson A. B. & Pelli D. G. QUEST: a Bayesian adaptive psychometric method.
490 *Perception & Psychophysics* 33, 113–120 (1983).
- 491 24. Meredith M. A. & Stein B. E. Visual, auditory, and somatosensory convergence on cells
492 in superior colliculus results in multisensory integration. *J Neurophysiol.* 56, 640-62
493 (1986).
- 494 25. Corbetta M., Akbudak E., Conturo T. E., Snyder A. Z., Ollinger J. M., Drury H. A. et
495 al. A common network of functional areas for attention and eye movements. *Neuron* 21,
496 761-773 (1998).
- 497 26. Grosbas M. H. & Paus T. Transcranial magnetic stimulation of the human frontal eye
498 field: effects on visual perception and attention. *J Cogn Neurosci.* 14, 1109-20 (2002).
- 499 27. Muggleton N. G., Juan C. H., Cowey A. & Walsh V. Human frontal eye fields and visual
500 search. *J Neurophysiol.* 89, 3340-3 (2003).
- 501 28. Moore T. & Armstrong K. M. Selective gating of visual signals by microstimulation of
502 frontal cortex. *Nature* 421, 370-373 (2003).
- 503 29. Silvanto J., Lavie N. & Walsh V. Stimulation of the human frontal eye fields modulates
504 sensitivity of extrastriate visual cortex. *J Neurophysiol.* 96, 941-5 (2006).
- 505 30. Quentin R., Chanes L., Vernet M. & Valero-Cabré A. Fronto-parietal anatomical
506 connections influence the modulation of conscious visual perception by high-beta
507 frontal oscillatory activity. *Cereb Cortex* 25, 2095-2101 (2015).
- 508 31. Ruff C. C., Blankenburg F., Bjoertomt O., Bestmann S., Freeman E., Haynes J. D. et al.
509 Concurrent TMS-fMRI and psychophysics reveal frontal influences on human
510 retinotopic visual cortex. *Curr Biol.* 16, 1479-1488 (2006).
- 511 32. Marshall T. R., O'Shea J., Jensen O. & Bergmann T. O. Frontal eye fields control
512 attentional modulation of alpha and gamma oscillations in contralateral occipitoparietal
513 cortex. *J Neurosci.* 35, 1638-1647 (2015).
- 514 33. Marshall T. R., Bergmann T. O. & Jensen O. Frontoparietal structural connectivity
515 mediates the top-down control of neuronal synchronization associated with selective
516 attention. *PLoS Biol.* 13, e1002272 (2015).
- 517 34. Hecht D. & Reiner M. Sensory dominance in combinations of audio, visual and haptic
518 stimuli. *Exp Brain Res.* 193, 307-14 (2009).

- 519 35. Donaldson P. H., Rineheart N. J. & Enticott P. G. Noninvasive stimulation of the
520 temporoparietal junction: A systematic review. *Neurosci Biobehav Rev.* 55, 547-572
521 (2015).
- 522 36. Karnath H. New insights into the functions of the superior temporal cortex. *Nat Rev*
523 *Neurosci.* 2, 568-576 (2001).
- 524 37. Friedrich F. J., Egly R., Rafal R. D. & Beck D. Spatial attention deficits in humans: A
525 comparison of superior parietal and temporal-parietal junction lesions.
526 *Neuropsychology* 12, 193-207 (1998).
- 527 38. Corbetta M. & Shulmann G. L. Control of goal-directed and stimulus-driven attention
528 in the brain. *Nat Rev Neurosci.* 3, 201-15 (2002).
- 529 39. Göschl F., Friese U., Daume J., König P. & Engel A. K. Oscillatory signatures of
530 crossmodal congruence effects: An EEG investigation employing a visuotactile pattern
531 matching paradigm. *Neuroimage* 116, 177-186 (2015).
- 532 40. Romero Y. R., Keil J., Balz J., Niedeggen M., Gallinat J., & Senkowski D. Alpha-Band
533 Oscillations Reflect Altered Multisensory Processing of the McGurk Illusion in
534 Schizophrenia. *Front Hum Neurosci.* 10, 41 (2016).
- 535 41. Wang W., Hu L., Cui H., Xie X. & Hu Y. Spatio-temporal measures of
536 electrophysiological correlates for behavioral multisensory enhancement during visual,
537 auditory and somatosensory stimulation: A behavioral and ERP study. *Neurosci Bull.*
538 29, 715–724 (2013).
- 539 42. Peng W., Hu L., Zhang Z. & Hu Y. Causality in the association between P300 and Alpha
540 event-related desynchronization. *PLoS One* 7, e34163 (2012).
- 541 43. Womelsdorf T., Johnston K., Vinck M. & Everling S. Theta-activity in anterior
542 cingulate cortex predicts task rules and their adjustments following errors. *Proc*
543 *NatlAcad Sci USA* 107, 5248-53 (2010).
- 544 44. Menon V. & Uddin L. Q. Saliency, switching, attention and control: a network model
545 of insula function. *Brain Struct Funct.* 214, 655-667 (2010).
- 546 45. Delorme A, & Makeig S. EEGLAB: an open source toolbox for analysis of single-trial
547 EEG dynamics. *J Neurosci Methods.* 134, 9-21 (2004).
- 548 46. Hipp J. & Siegel M. Dissociating neuronal gamma-band activity from cranial and ocular
549 muscle activity in EEG. *Front Hum Neurosci.* 7, 338 (2013).
- 550 47. Hassler U., Trujillo-Barreto N. & Gruber T. Induced gamma band responses in human
551 EEG after the control of miniature saccadic artifacts. *Neuroimage* 57, 1411-1421
552 (2011).
- 553 48. Pascual-Marqui R. D., Lehmann D., Koukkou M., Kochi K., Anderer P., Saletu B. et al.
554 Assessing interactions in the brain with exact low-resolution electromagnetic
555 tomography. *Philos Trans A Math Phys Eng Sci.* 369, 3768-84 (2011).
- 556 49. Nolte G. & Dassios G. Analytic expansion of the EEG lead field for realistic volume
557 conductors. *Phys Med Biol.* 50, 3807-23 (2005).
- 558 50. Desikan R. S., Segonne F., Fischl B., Quinn B. T., Dickerson B. C., Blacker D. et al. An
559 automated labeling system for subdividing the human cerebral cortex on MRI scans into
560 gyral based regions of interest. *Neuroimage* 31, 968-980 (2006).
- 561 51. Maris E. & Oostenveld R. Nonparametric statistical testing of EEG- and MEG-data. *J*
562 *Neurosci Methods* 164, 177-90 (2007).

a**attentional focus**

visual-tactile

audio-visual

tactile



incongruent

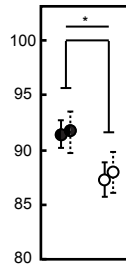


visual

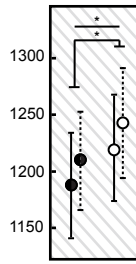


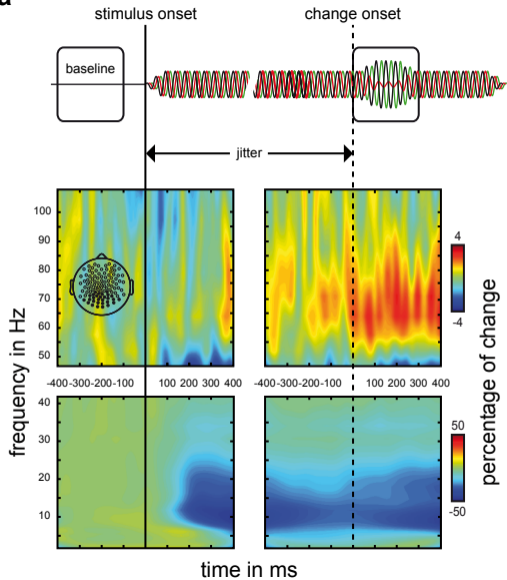
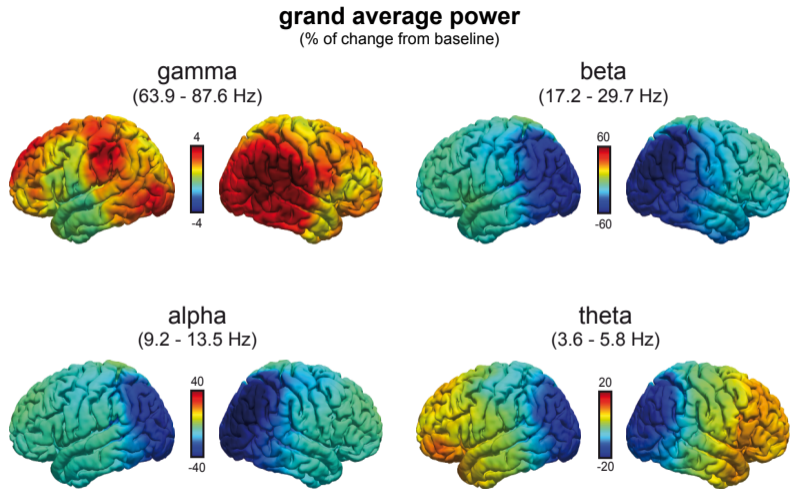
congruent

audio

**b****stimulus configurations****FC**
(fully congruent)**DC**
(distracted congruent for VT)**DC**
(distracted congruent for AV)**INC**
(incongruent for VT and AV)**c****ACC**

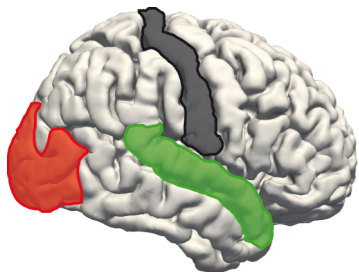
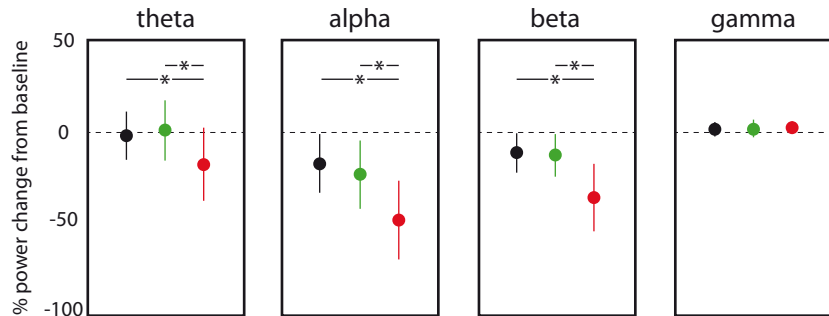
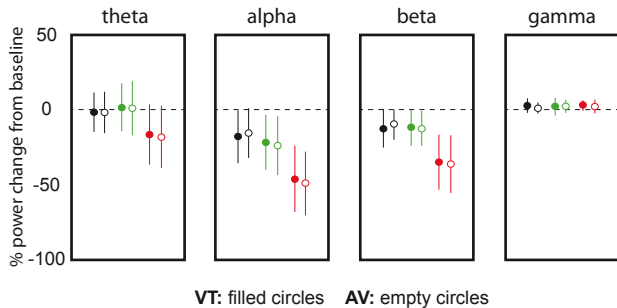
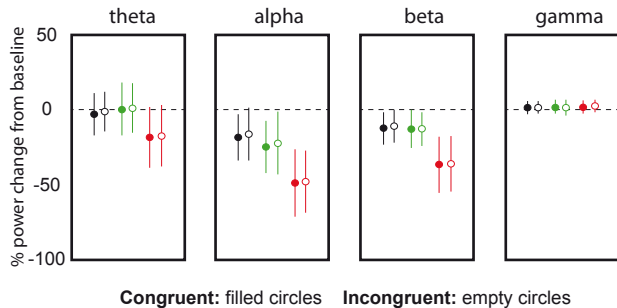
● VT ○ AV

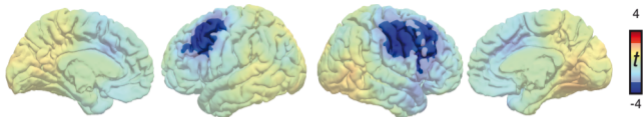
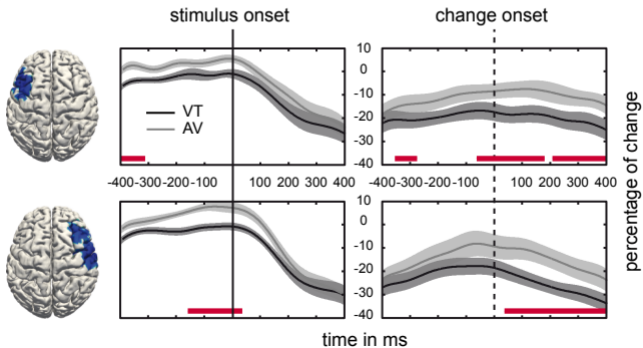
— congruent
..... incongruent**d****RT**— congruent
..... incongruent

a**b**

a

regions of interest (ROIs)

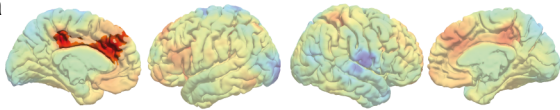
**b**effect of *ROI***c**no effect of *ATTENTION***d**no effect of *CONGRUENCE*

a**alpha: VT - AV****b**

theta

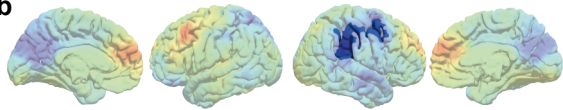
alpha

a

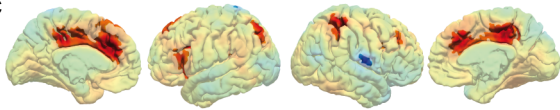


Con - Inc

b

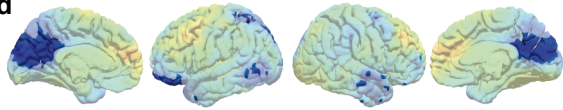


c



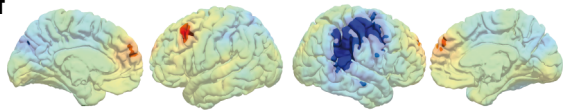
FC - Inc

d



DC - Inc

f



-4 *t-values* 4